

MINIREVIEW

[View Article Online](#)
[View Journal](#) | [View Issue](#)

Cite this: *Polym. Chem.*, 2020, **11**, 6413

Bioinspired structural color nanocomposites with healable capability

Lianbin Zhang, , Miaomiao Li, Quanqian Lyu and Jintao Zhu *

As fascinating biological functions of many organisms, structural colors and healable features play crucial roles in the survival of many organisms. Inspired by these features, healable structural color nanocomposites that integrate the photonic structure and healable polymeric materials have been attracting growing attention recently. Healable structural color nanocomposites can effectively heal their damage and ensure sustainable optical and mechanical properties of the functional materials, demonstrating extensive application prospects in visual sensors, colorful painting, and anti-counterfeiting. In this minireview, from the perspective of the construction strategies, we summarize the recent development of the healable structural color nanocomposites as well as the existing challenges in this emerging area. We hope that this minireview will inspire future research efforts to push forward the studies and applications of healable structural color nanocomposites.

Received 31st July 2020,
Accepted 20th September 2020

DOI: 10.1039/d0py01096k

rsc.li/polymers

1. Introduction

In nature, many organisms, such as butterfly wings, chameleon skin, bird feathers, and opals, exhibit colorful appearances, which are known as structural colors.^{1–4} Unlike molecular pigments, whose colors are based on the absorption of light, structural colors originate from the interaction of inci-

dent light with the micro- and nanostructures.^{1–4} Structural color is one of the most important characteristics of photonic crystals (PCs).^{5–7} PC materials possess periodic structures with different refractive indexes and can regulate the transmission of the incident light *via* diffraction and scattering. The pioneering research on structural colors dates back to the early 17th century by Hooke and Newton and a deeper understanding was then achieved by the establishment of electromagnetic theory and observation of the nanostructure by electron microscopy.^{2,8} Besides the structural color, PCs also demonstrate many important functional properties, including tunable photonic bandgaps, photon localization effects, and

Key Laboratory of Material Chemistry for Energy Conversion and Storage of Ministry of Education (HUST), and State Key Laboratory of Materials Processing and Die & Mold Technology, Huazhong University of Science and Technology (HUST), Wuhan 430074, China. E-mail: jtzhu@mail.hust.edu.cn



Lianbin Zhang

Lianbin Zhang received his B.Sc. degree in polymer material and engineering in 2005 and Ph.D. degree in polymer chemistry and physics in 2010, both from Jilin University, China. Then, he worked as a postdoctoral researcher and research scientist from 2010 to 2016 in the Hongkong University of Science and Technology and King Abdullah University of Science and Technology, respectively. In Oct. 2016, Dr Zhang joined the

School of Chemistry and Chemical Engineering at HUST as a full professor. His research interests focus on supramolecular materials and responsive photonic materials.



Miaomiao Li

Miaomiao Li is currently a Ph.D. candidate under the supervision of Prof. Lianbin Zhang and Jintao Zhu, at the School of Chemistry and Chemical Engineering, HUST. Her research interests are on responsive photonic materials.

others.^{9–12} These features ensure PC materials with many promising applications, ranging from optical displays and anti-counterfeiting techniques to sensors;^{11,13–20} especially, for the tunable photonic bandgap induced by external stimuli, the structural colors of the photonic materials can be directly observed by the naked eye, providing a convenient route for signal readout in visual sensors.^{10,21–25}

In general, PC materials with periodic structures can be obtained by many well-established strategies, including photolithography,²⁶ assembly of block copolymers,^{27–29} cellulose nanocrystals,^{30–32} and colloidal particles;^{16,33} especially, colloidal PCs constructed by the assembly of monodisperse nanoparticles (NPs) have attracted particular interest due to the unique advantages of facile and large-scale fabrication, low costs, and readily tunable bandgaps.¹⁶ A rich variety of colloidal particles with tunable sizes and refractive indexes have been exploited in the construction of colloidal PCs.²⁵ Furthermore, by utilizing colloidal PCs as templates, inverse opal structures can also be obtained by infusion of the precursors, followed by the solidification and removal of the colloidal templates.³⁴ The resulting cavities in inverse opal structures greatly expand the applications of colloidal PCs.^{35,36}

When being applied in daily life, colloidal PCs are likely to be handled *via* physical mechanisms, which in turn can bring the possibility of damage to the delicate periodic nanostructures, leading to the failure of the optical and/or structural properties.^{37,38} Therefore, improving the mechanical strength of colloidal PC materials has been one of the critical aspects to ensure the durability and stability of PCs. To this end, several strategies have been employed for the construction of mechanically robust colloidal PCs. For example, cross-linking of colloidal crystals *via* a thermal or chemical process can greatly improve the connection between the individual

NPs.^{38–42} Structural color nanocomposites which are obtained through the incorporation of the colloidal PCs into polymeric matrices have also been developed to enhance the durability of the PCs since soft polymeric materials with intrinsic flexibility provide the composite PCs with the capability of resisting mechanical deformation, maintaining the integrity of the PCs.^{21,43–46} Furthermore, the introduction of the polymeric matrix also endows the PCs with unique functionalities. For instance, structural color nanocomposites can be used as a visual strain sensor with adhesive capability.^{40,47} Our group has also utilized responsive hydrogels to incorporate assembled Fe₃O₄ colloidal particles and constructed chemical and force structural color sensors.^{48–50} Although these strategies have been demonstrated to be effective in improving the reliability and functionality of PC materials, challenges, including the large deformation and the abrasion of the surface of the PCs, remain and limit their applications.

To address the failure or damage of the structures and the functions, nature once again provides us pioneering solutions *via* autonomous recovery of organisms after being wounded, which is known as healable capability.^{51,52} Inspired by this fascinating capability, recent decades have witnessed the rapid development of healable materials.^{51,52} Great efforts have been made for the development of polymeric materials based on reversible covalent bonds or supramolecular interaction, and these healable polymeric materials have been successfully employed in the construction of healable nanocomposite materials for use as electronic devices.^{53–57} Recently, structural color nanocomposites with healable capability have also been obtained with healable polymeric materials, and it has been shown that the introduction of the healable polymeric materials can effectively ensure the reliability and the long-term use of the PCs after severe damage. Furthermore,



Quanqian Lyu

Quanqian Lyu is currently a Ph.D. candidate under the supervision of Prof. Lianbin Zhang and Jintao Zhu, at the School of Chemistry and Chemical Engineering, HUST. His research interests focus on responsive photonic materials.



Jintao Zhu

Jintao Zhu received his Ph.D. degree from Changchun Institute of Applied Chemistry, Chinese Academy of Sciences. He then worked as a postdoctoral research fellow at the University of Alberta and the University of Massachusetts Amherst. Since 2009, he has been appointed as a professor at the School of Chemistry and Chemical Engineering, HUST. Dr Zhu is serving as an editor of Macromolecular Research. His current interests involve self-assembled polymers and nanoparticles for responsive nanophotonics, healing materials, memory devices, and immunotherapy. Dr Zhu is a recipient of Fellow of the Royal Society of Chemistry (2020), China National Funds for Distinguished Young Scholar (2015), and Chinese Chemical Society Youth Awards (2013).

additional functions such as mechanochromic performance, easy-recycling, and biocompatibility can be integrated into the composites, greatly expanding their applications.^{58–61} In this minireview, we aim to present a comprehensive overview of the state of the art of structural color nanocomposites with healable capability. Yet, the review is by no means meant to be exhaustive; instead, we try to give a focused and critical review of this burgeoning field using a limited number of selected examples. Critical challenges and outlook of structural color nanocomposites are also discussed.

2. Design principles of structural color nanocomposites with healable capability

Structural color nanocomposites can be obtained by the combination of ordered nanostructures with polymeric materials, and conventionally, they can be usually obtained by (1) assembly of colloidal particles, followed by the infiltration of a polymerizable precursor and solidification process,^{13,44,62–64} or (2) assembly of colloidal particles in the presence of the monomers, followed by a polymerization process.^{22,48,65–67} Due to the facile and cost-effective preparation, a wide range of colloidal particles, such as silica NPs (SiO_2 NPs), polystyrene NPs (PS NPs), Fe_3O_4 NPs, and others, are usually chosen as building blocks for the construction of photonic structures with an opal structure by the assembly strategy.¹⁶ Besides, the structural color nanocomposites can also be obtained by replicating the assembled opal structures, which is known as the inverse opal structure, by a series of preparation steps, such as fabrication of the template, infusion of the polymerizable monomer, followed by polymerization of the monomer, and removal of the colloidal template.⁶⁸

Healable polymeric materials are polymers constructed by dynamic reversible connections, including reversible covalent bonding, such as imine bonds, boronate ester, acylhydrazones, or supramolecular interactions, such as hydrogen bonding,

metal coordination, ionic and hydrophobic interactions, and host-guest interactions.^{51,52,57,69–75} Since these connections in the polymeric materials can be broken and then reformed, these materials can maintain the integrity of the structure and restore their mechanical properties after being damaged.⁶⁹ When these healable polymeric materials are introduced into the colloidal PC structures, it is anticipated that the healability can be imparted to the resultant structural color nanocomposites. Considering the functionalities of the polymers used, these healable structural color nanocomposites will find more applications and attract more attention. Currently, by using healable polymers, three strategies have been mainly adopted to obtain the structural color nanocomposites with healable capability (Fig. 1): (1) self-assembly of colloidal particles tethered with polymer chains with dynamic reversible connections;⁷⁶ (2) introduction of healable polymeric materials (*i.e.*, polymers or polymerizable materials) into preformed periodic nanostructures (*i.e.*, ordered opal structure and inverse opal scaffold structure);^{60,65,77–81} (3) self-assembly of colloidal particles with healable polymeric materials.^{58,59,61,82,83} These dynamic reversible bonds in the structural color nanocomposites endow the materials with healable capability. Therefore, the following sections will be organized according to the recent progress and the structural and matrix characteristics of the resultant structural color nanocomposites as shown in Fig. 1.

2.1 Self-assembly of colloidal particles tethered with polymer chains

In 2015, Guan *et al.* for the first time reported healable structural color nanocomposites by self-assembly of polymer-tethered NPs.⁷⁶ In their work, monodisperse SiO_2 NPs were first functionalized with an atom transfer radical polymerization (ATRP) initiator and then polyacrylate amide (PA-amide) brushes were grafted with large quantities and tunable lengths. Through a simple solution casting and hot pressing, structural color nanocomposites can be obtained (Fig. 1(A)). The dynamic nature of hydrogen bonding between the PA-amide brushes grafted on NPs affords healing properties to

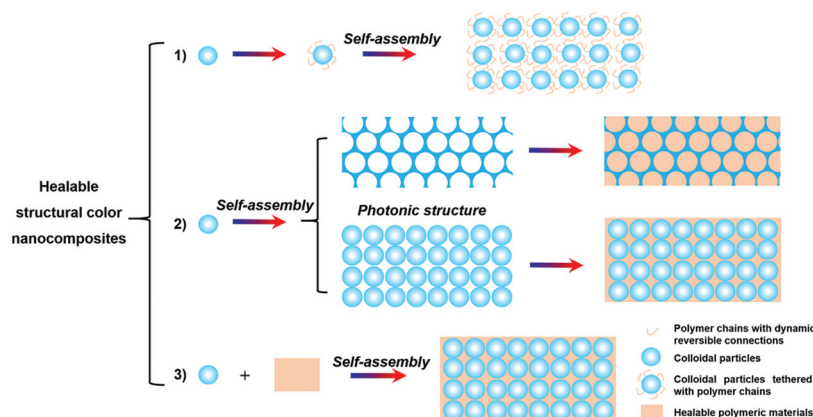


Fig. 1 Schematic illustration for the strategies for generating structural color nanocomposites with healable capability.

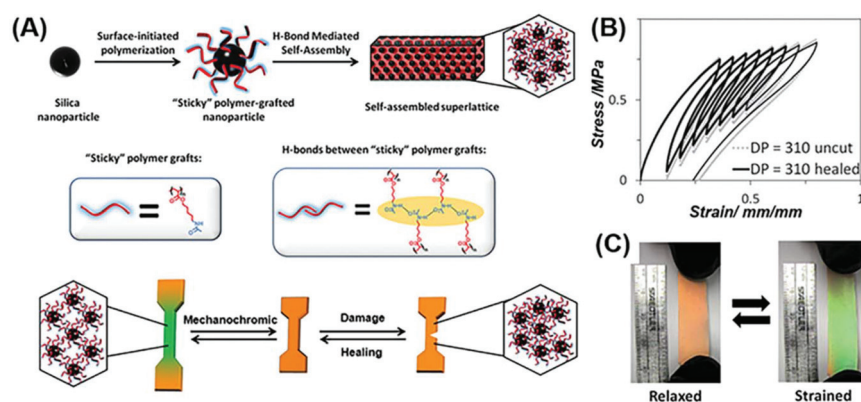


Fig. 2 Healable structural color nanocomposites *via* self-assembly of colloidal particles tethered with polymer chains. (A) The preparation of polymer grafted NPs by the surface-initiated ATRP method and their mechanochromic and healing performance. (B) Fracture toughness of the resultant structural color nanocomposites before and after healing. Strain rate = 1 mm min⁻¹ and relax rate = 1 mm min⁻¹. (C) The photographs of healable structural color nanocomposites under the strained and relaxed conditions. Reproduced from ref. 76 with permission from John Wiley and Sons, copyright 2015.

the self-assembled nanocomposites. Due to the flexible nature and the high grafting density of the PA-amide brushes, the nanocomposites show a good stretchable property, and the structural color of the nanocomposites can be tuned from red to green when being relaxed and strained (Fig. 2(B) and (C)). This work provides a simple, scalable approach to prepare healable structural color nanocomposites possessing high structural orders as well as robust and dynamic mechanical properties.

2.2 Introduction of healable polymeric materials into preformed periodic nanostructures

2.2.1 Infusion of healable polymeric materials into an ordered inverse opal structure. Although the polymer-tethered NPs can realize the healing of the structure and optical performance, the preparation of such functionalized NPs necessitates the complicated synthesis. Facile preparation of the structural color nanocomposites is highly desirable. Compared with the self-assembly of the functionalized NPs, the infusion of healable polymeric materials into a previously formed periodic nanostructure by the commonly employed building blocks for the preparation of the structural color nanocomposite will be more general. In 2017, Zhao reported the preparation of healable structural color hydrogels by infusing a healable protein hydrogel into a frequently used inverse opal scaffold.⁷⁸ The inverse opal scaffolds were obtained by polymerizing a methacrylated gelatin (GelMA) hydrogel to replicate a self-assembled silica NP-based opal template (Fig. 3(A)). Then, a glutaraldehyde cross-linked bovine serum albumin (BSA) hydrogel with enzyme additives of glucose oxidase (GOX) and catalase (CAT) was filled in the nanovoids of inverse opal scaffolds to obtain the healable hydrogel-based structural color nanocomposites. The periodically ordered structure of the polymerized GelMA inverse opal scaffolds endowed the hydrogel nanocomposite with a bright structural color. The reversible imine covalent connection in the filled protein hydrogel endowed the compo-

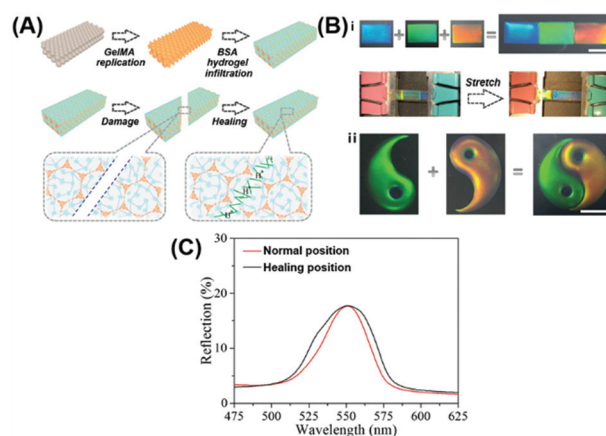


Fig. 3 Healable structural color nanocomposite *via* an infusion of healable polymeric materials into an ordered inverse opal structure. (A) Preparation of the structural color hydrogel material and its healing process. (B) Optical images of the healing process of structural color hydrogels. The scale bars for (i) and (ii) are 5 mm. (C) Reflection spectra of the original and healed structural color hydrogel at the damage position. Reproduced from ref. 78 with permission from the National Academy of Sciences, copyright 2017.

site structural color hydrogel with the healability. Furthermore, the acidic environment that was created by the glucose in the presence of glucose oxidase can promote the dynamic exchange reaction of imine bonds. Therefore, the healing behavior of the structural color hydrogel can be achieved by coating glucose in the damaged position. Based on the healing behavior of the nanocomposites, the resultant hydrogel segments with different structural colors and patterns can be integrated to form an intact pattern by adding glucose to the joint (Fig. 3(B)). The invariable optical properties of the structural color hydrogel before and after healing, as shown in Fig. 3(C), demonstrated that it provided an effective strategy for the construction of the hydrogel-based

structural color nanocomposites with healable capability. In addition, the composite hydrogels were shown to have the capability to resist external stretching forces, and with the stretching strains, the lattice spacing in the materials decreased, blue-shifting their structural color. In their following studies, Zhao *et al.* infused a mixture of a hydrogel with reversible phase transition function and graphene oxide (GO) into a polymeric inverse scaffold.⁷⁷ Due to the large size, GO nanosheets cannot get into the nanocavities; instead, they covered the upper layer to strengthen the color contrast with a dark background. In addition, the photothermal conversion capability of GO makes the structural color hydrogel show light-controlled healing behavior. These features of the healable structural color hydrogel could broaden the scope of designability for photonic devices, and promote the development of structural color materials (*e.g.*, anti-counterfeiting labels and visual sensors).

2.2.2 Introduction of the healable polymeric materials into a preformed ordered opal structure. Besides inverse opal structures, the periodic nanostructure with an opal structure is more convenient to be realized by the assembly of colloidal particles. Yin and coworkers reported the preparation of healable structural color hydrogels by using poly (1-vinyl-2-pyrrolidinone-*co*-acrylamide) (poly (NVP-*co*-AAM)) modified with *O*-carboxymethyl chitosan (*O*-CMC) as a matrix material, which has good mechanical properties and elasticity, and silica-coated Fe_3O_4 NPs ($\text{Fe}_3\text{O}_4@\text{SiO}_2$ NPs) as building blocks under the magnetic field (Fig. 4(A)).⁸¹ The reversible hydrogen bonds between the plentiful carboxyl, amino, and hydroxyl functional groups could impart the nanocomposite hydrogel with healable capability. As shown in Fig. 4(B) (i–iv), when the resultant hydrogel columns with different colors were put in contact with each other with the two surfaces being in physical contact for a period of time, the hydrogen bonding could rapidly form and connect the two separated hydrogel columns. The joined hydrogel column can be stretched under different strain conditions without any cracks. Moreover, the stress–strain curves

of hydrogel nanocomposites healed for 24 h shown in Fig. 4(C) further confirmed that polymer networks of the hydrogel nanocomposite had a good healable capability. A similar structural color hydrogel with healability was also demonstrated by Zhao *et al.* using the $\text{Fe}_3\text{O}_4@\text{SiO}_2$ NPs and gelatin hydrogels, and they further showed that the magnetic NPs can absorb near-infrared light and generate heat, prompting the healing of the hydrogels.⁶⁰ In addition, these hydrogels also demonstrated excellent biocompatibility and can be promising in many biological applications in cell engineering and biological engineering.

2.3 Self-assembly of colloidal particles with healable polymeric materials

Conventionally, structural color nanocomposites were obtained by the self-assembly of colloidal particles, followed by the introduction of polymeric materials, which is usually a multi-step process. One-step preparation of structural color nanocomposites will be highly favorable for their large-scale production and practical applications. Recently, attempts have been made to produce healable structural color nanocomposites, especially with the recently developed angle-independent structural color nanocomposites.^{58,59,61,82,83} Angle-independent structural color, which is different from the structural color of the PC with long-range ordered periodic nanostructures, arises from the interaction of amorphous or short-range ordered colloidal arrays and visible light.^{84,85} PC materials with angle-independent structural color exhibit invariable color when being viewed from a different direction and are beneficial for the precise determination of colors in colorimetric sensors.¹ On the other hand, compared with the well-defined periodic PCs, the amorphous or short-range ordered nanostructures can be readily and conveniently obtained, and thus PCs with short-range ordered nanostructures have attracted increasing attention;^{45,86} especially when polymer materials are introduced into the assembly process of colloidal particles, which accordingly can affect the

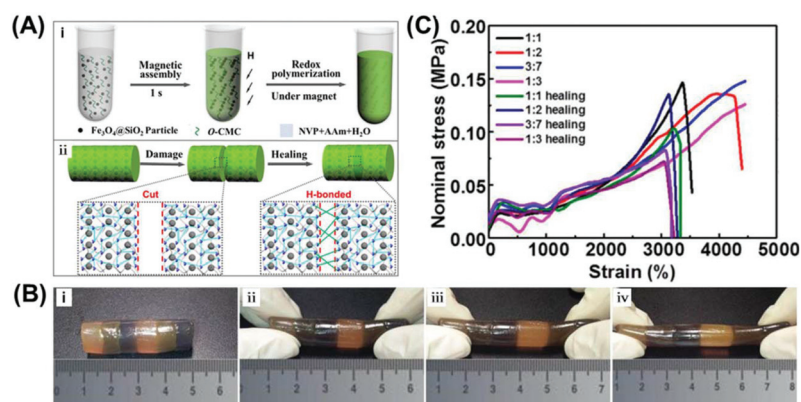


Fig. 4 Healable structural color nanocomposites *via* an infusion of healable polymeric materials into an ordered opal structure. (A) Preparation of the structural color hydrogel material (i) and its healing mechanism (ii). (B) Photographs of the constructed healable structural color hydrogel column with different colors under different stretching (i–iv) deformations. (C) Stress–strain curves for original and healed hydrogels. Reproduced from ref. 81 with permission from the American Chemical Society, copyright 2020.

arrangement of the NPs, structural color nanocomposites with angle-independent structural colors can be obtained.⁸⁷

2.3.1 Healable organogel-based structural color nanocomposites. Yao *et al.* first prepared healable structural color organogels by combining the colloidal PCs and healable supramolecular organogels.⁵⁹ As illustrated in Fig. 5(A) and (B), the healable supramolecular polymer (IPDI-PDMS) was first synthesized through the condensation of amino-terminated poly(dimethylsiloxane) (amino-PDMS) and isophorone diisocyanate (IPDI), and then was co-assembled with oleophilic SiO₂ NPs, carbon black (CB), and silicone oil. After solvent evaporation, SiO₂ NPs were arranged into a short-range ordered photonic structure in the gelatinization polymer matrix and structural color organogels were achieved. These dynamic and reversible hydrogen bonds in the gelatinization polymer matrix could hinder the ordered arrangement of NPs and endow the organogel nanocomposites with angle-independent structural color and healable capability as shown in Fig. 5(C). Additionally, compared to the healable hydrogel materials, the organogel-based healable materials showed unique features of interfacial slipperiness and water repellency, which promote the outdoor application of the structural color materials (Fig. 5(D)).

2.3.2 Healable elastomer-based structural color nanocomposites. Compared with gel materials, solvent-free elastomers have attracted much attention due to their high mechanical strength, stability, and elasticity. To ensure sustainable optical and mechanical properties and improve the mechanical strength, the elastomer-based healable structural color materials can be realized by combining the photonic structure with a healable elastomer or polymer. Our group prepared the structural color elastomer with healability through the co-assembly of SiO₂ NPs and a supramolecular elastomer based on metal coordination interaction between amino-PDMS and cerium ions (Ce^{III}).⁵⁸ SiO₂ NPs arranged into photonic structures within the polymer matrix, giving rise to the structural

colors, and the introduced metal coordination interaction in the polymeric matrix provided healable capability (Fig. 6(A)). Elastomers with different bright structural colors can be clearly observed by the naked eye through adjusting the size of incorporated NPs and display angle-independent structural colors (Fig. 6(B) and (C)). Compared with gel materials, the superelastic properties and stability of the elastomer endow the structural color materials with an excellent color shifting and recovery performance when stretching and bending the elastomer, similar to chameleon skin (Fig. 6(D)). Furthermore, as shown in Fig. 6(E) and (F), such structural color elastomers can heal the surface scratches and cuts because of the flexi-



Fig. 6 Healable structural color elastomer nanocomposite. (A) Illustration showing the structural design of healable structural color elastomer nanocomposites and the reversible interactions between Ce(III) and amino-PDMS chains. The photographs of structural color elastomers prepared from SiO₂ NPs with different sizes on a black substrate at a viewing angle of 0° (B) and 60° (C). (D) The color change of a red-colored elastomer nanocomposite with different stretching strains. Optical microscopy images of an abraded elastomer nanocomposite before (E) and after (F) healing at room temperature for 48 h. Reproduced from ref. 58 with permission from John Wiley and Sons, copyright 2019.



Fig. 5 Healable structural color organogel nanocomposites. (A) Synthesis of the healable supramolecular polymer (IPDI-PDMS). (B) Schematic illustration of the fabrication of the healable structural color organogel by co-assembly of SiO₂ NPs, CB, and healable IPDI-PDMS polymer gel with silicone oil. (C) The optical images of a cut (left) and healed (right) structural color organogel. The sample area was 1.5 cm × 1.5 cm. (D) Photographs of the droplet sliding on an inclined organogel nanocomposite surface with a healing process of cut damage over time. The droplet was pinned at the damaged area and continued sliding when the nanocomposite healed itself. Reproduced from ref. 59 with permission from John Wiley and Sons, copyright 2017.

bility of the PDMS matrix and reversible coordination interaction, ensuring long-term usage in the fields of wearable devices, optical coating, and visual force sensing. By using a similar strategy, other healable polymeric materials including polyborosiloxane and poly(ethylene glycol)-based elastomers have also been employed for the construction of the healable structural color elastomers to improve the healing capability and environmentally friendly properties.^{61,83}

When the structural color elastomer nanocomposite is used in visual sensors and color coating, the structural color and spectrum responsiveness are critically important for determining the color. Recently, our group prepared a healable elastomer nanocomposite with high color saturation and broad-

spectrum responsiveness by incorporating the carbon-coated Fe_3O_4 NPs ($\text{Fe}_3\text{O}_4@\text{C}$ NPs) into an amino-terminated PDMS polymer through supramolecular interactions (Fig. 7(A)).⁸² Due to a high refractive index of ~ 1.9 and broad-band light absorption of $\text{Fe}_3\text{O}_4@\text{C}$ NPs, the resultant elastomer prepared from $\text{Fe}_3\text{O}_4@\text{C}$ NPs displayed visible colors even when being placed on a white substrate (Fig. 7(B)). More importantly, under the irradiation with laser or sunlight, the resultant elastomer showed improved healing behavior for the damage as shown in Fig. 6(C). The inherent photothermal properties of $\text{Fe}_3\text{O}_4@\text{C}$ NPs enable the elastomer material to absorb light (laser and sunlight) and convert it into heat, accelerating the healing performance. Besides, through adjusting the volume fraction of $\text{Fe}_3\text{O}_4@\text{C}$ NPs, the enlarged interparticle distance and tensile properties endowed the elastomer with broad-spectrum responsiveness and excellent recovery under a large strain. As shown in Fig. 7(D), when being stretched, the structural color of the elastomer changed from red to blue. After release, it could almost recover to its initial color. The color change in the stretching and releasing processes was reversible and recoverable under 75% stretching strain, indicating excellent prospects in the visual sensor.



Fig. 7 Healable structural color elastomer nanocomposite with high color saturation and broad-spectrum responsiveness. (A) Illustration showing the structural design of the structural color elastomer nanocomposite and the reversible interactions between $\text{Fe}_3\text{O}_4@\text{C}$ NPs and amino-PDMS chains. (B) Photographs of structural color elastomers prepared from $\text{Fe}_3\text{O}_4@\text{C}$ NPs with different sizes on a white substrate at a viewing angle of 0° and 60° . (C) Optical microscopy images of a cut (i) and abraded (iii) elastomer nanocomposite before (i and iii) and after (ii and iv) healing under the irradiation with laser and sunlight for different healing times. (D) Photographs of a red-colored elastomer nanocomposite under stretching (top) and releasing (bottom) at various strains. Reproduced from ref. 82 with permission from John Wiley and Sons, copyright 2020.

3. Summary and outlook

Inspired by the structural color and the autonomous recovery capabilities of organisms, structural color nanocomposites with healable capability integrate the two fascinating features in nature and represent the state-of-the-art nanocomposite materials for advanced applications in visual sensors, colorful painting, anti-counterfeiting, and others. This minireview summarizes the recently developed construction strategies for the structural color nanocomposites with healable capability (Table 1). The healability of the structural color nanocomposites ensures the reliability and the durability of the colorful materials in practical applications and will greatly contribute to the needs of a sustainable society. Although considerable progress has been achieved in the past years, significant challenges and barriers remain between the *status quo*

Table 1 Healing performance of the structural color nanocomposites

Construction strategy	Healing mechanism	Healing conditions	Healing efficiency	Ref.
(1)	Hydrogen bonding	At room temperature	—	76
(2)	Imine bond	3 h at 4°C and the stimulation of glucose	—	78
	Phase transformation	Laser irradiation	$\sim 83\%^a$	77
	Hydrogen bonding	24 h at room temperature	$\sim 73\%^a$	81
	Phase transformation	Under near-infrared irradiation or external magnetic fields	$\sim 60\%^a$	60
(3)	Hydrogen bonding	30 s at room temperature	$100\%^c$	59
	Metal-ligand coordination	48 h at 60°C	$80\%^b$	58
	Hydrogen bonding	2 h under near-infrared irradiation	$53\%^a$	82
	Boronic ester	20 min at room temperature	$100\%^a$	61
	Hydrogen bonding	90 min at room temperature	$100\%^a$	83

(1),(2),(3) Construction strategies of structural color nanocomposites shown in Fig. 1. ^a Healing efficiency obtained from the recovery rate of maximum stress. ^b Healing efficiency obtained from the recovery rate of maximum strain. ^c Healing efficiency obtained from the recovery rate of storage modulus.

and the practical applications of the healable structural color nanocomposites. First, similar to that of the healable polymeric materials, the mechanical robustness and healability of structural color nanocomposites are opposing. Although the introduction of the inorganic NPs can improve the mechanical strength of the structural color nanocomposites, they also can restrict the movements of the polymer chain, suppressing the healability. Therefore, a balance between the mechanical robustness and healability should be carefully considered when designing the ideal structural color nanocomposites. On the other hand, although the self-assemblies of colloidal particles with healable polymeric materials are beneficial to the large-scale production of structural color nanocomposites with angle-independent structural color, the realization of well-ordered nanocomposites through such a process is still highly challenging. The introduction of the polymer in the assembly process usually leads to an amorphous structure because the presence of the viscous polymeric matrix will trap the NPs into the metastable state by inhibiting the entropy-driven self-assembly of NPs, which usually results in a short-range ordered structure. Such an issue might be solved by carefully optimizing the interaction between the NPs and the polymer matrix and the chemistry of the polymers. Looking at the future, the structural color nanocomposites are still in their infancy, and we believe that with the continuous development of healable materials, new structural color nanocomposites and construction strategies will be reported, which will undoubtedly achieve their unprecedented performance and unproved potential in the future materials.

Conflicts of interest

There are no conflicts of interest to declare.

Acknowledgements

We acknowledge the funding from the Key R&D Program of Ministry of Science and Technology (2018YFA0209200), National Natural Science Foundation of China (51973075, 21704029, and 51525302), Ministry of Education Key Laboratory for the Synthesis and Application of Organic Functional Molecules of Hubei University, and Program for HUST Academic Frontier Youth Team (2015-01).

Notes and references

- S. Kinoshita, S. Yoshioka and J. Miyazaki, *Rep. Prog. Phys.*, 2008, **71**, 76401–76430.
- S. L. Burg and A. J. Parnell, *J. Phys.: Condens. Matter*, 2018, **30**, 413001–413030.
- Y. Zhao, Y. Zhao, S. Hu, J. Lv, Y. Ying, G. Gervinskis and G. Si, *Materials*, 2017, **10**, 944–957.
- C. G. Schafer, C. Lederle, K. Zentel, B. Stuhn and M. Gallei, *Macromol. Rapid Commun.*, 2014, **35**, 1852–1860.
- T. Hellweg, *Angew. Chem., Int. Ed.*, 2009, **48**, 6777–6778.
- L. Shang, W. Zhang, K. Xu and Y. Zhao, *Mater. Horiz.*, 2019, **6**, 945–958.
- M. Poutanen, G. Guidetti, T. I. Groschel, O. V. Borisov, S. Vignolini, O. Ikkala and A. H. Groschel, *ACS Nano*, 2018, **12**, 3149–3158.
- Z. Wang and Z. Guo, *Chem. Commun.*, 2017, **53**, 12990–13011.
- S. Wu, H. Xia, J. Xu, X. Sun and X. Liu, *Adv. Mater.*, 2018, **30**, 1803362.
- G. Isapour and M. Lattuada, *Adv. Mater.*, 2018, **30**, 1707069.
- Q. Zhang, M. J. Serpe and S. M. Mugo, *Polymers*, 2017, **9**, 436–450.
- K. Szendrei, A. Jiménez-Solano, G. Lozano, B. V. Lotsch and H. Míguez, *Adv. Opt. Mater.*, 2017, **5**, 1700663.
- H. Fudouzi and T. Sawada, *Langmuir*, 2006, **22**, 1365–1368.
- A. Chiappini, L. T. N. Tran, P. M. Trejo-Garcia, L. Zur, A. Lukowiak, M. Ferrari and G. C. Righini, *Micromachines*, 2020, **11**, 290–314.
- W. Hong, Z. Yuan and X. Chen, *Small*, 2020, **16**, 1907626.
- J. Hou, M. Li and Y. Song, *Angew. Chem., Int. Ed.*, 2018, **57**, 2544–2553.
- M. Huang, S.-G. Lu, Y. Ren, J. Liang, X. Lin and X. Wang, *J. Text. Inst.*, 2019, **111**, 756–764.
- M. Pan, L. Wang, S. Dou, J. Zhao, H. Xu, B. Wang, L. Zhang, X. Li, L. Pan and Y. Li, *Crystals*, 2019, **9**, 417–438.
- P. Wu, J. Wang and L. Jiang, *Mater. Horiz.*, 2020, **7**, 338–365.
- Y. Qi, L. Chu, W. Niu, B. Tang, S. Wu, W. Ma and S. Zhang, *Adv. Funct. Mater.*, 2019, **29**, 1903743.
- T. Ito, C. Katsura, H. Sugimoto, E. Nakanishi and K. Inomata, *Langmuir*, 2013, **29**, 13951–13957.
- G. H. Lee, T. M. Choi, B. Kim, S. H. Han, J. M. Lee and S. H. Kim, *ACS Nano*, 2017, **11**, 11350–11357.
- R. Zhang, Q. Wang and X. Zheng, *J. Mater. Chem. C*, 2018, **6**, 3182–3199.
- Y. Takeoka, *J. Mater. Chem. C*, 2013, **1**, 6059–6074.
- J. Ge and Y. Yin, *Angew. Chem., Int. Ed.*, 2011, **50**, 1492–1522.
- C. Hsu, Z. Xu, C. Liao and X. Wang, *Adv. Opt. Mater.*, 2019, **7**, 1900846.
- A. L. Liberman-Martin, C. K. Chu and R. H. Grubbs, *Macromol. Rapid Commun.*, 2017, **38**, 1700058.
- T. Zhang, J. Yang, X. Yu, Y. Li, X. Yuan, Y. Zhao, D. Lyu, Y. Men, K. Zhang and L. Ren, *Polym. Chem.*, 2019, **10**, 1519–1525.
- D. P. Song, C. Li, W. Li and J. J. Watkins, *ACS Nano*, 2016, **10**, 1216–1223.
- H. Chen, A. Hou, C. Zheng, J. Tang, K. Xie and A. Gao, *ACS Appl. Mater. Interfaces*, 2020, **12**, 24505–24511.
- J. Chen, L. Xu, X. Lin, R. Chen, D. Yu, W. Hong, Z. Zheng and X. Chen, *J. Mater. Chem. C*, 2018, **6**, 7767–7775.
- C. Boott, A. Tran, W. Hamad and M. MacLachlan, *Angew. Chem.*, 2020, **59**, 226–231.
- P. Liu, L. Bai, J. Yang, H. Gu, Q. Zhong, Z. Xie and Z. Gu, *Nanoscale Adv.*, 2019, **1**, 1672–1685.

- 34 M. Quan, B. Yang, J. Wang, H. Yu and X. Cao, *ACS Appl. Mater. Interfaces*, 2018, **10**, 4243–4249.
- 35 Y. Ohtsuka, T. Seki and Y. Takeoka, *Angew. Chem., Int. Ed.*, 2015, **54**, 15368–15373.
- 36 J. Wang, Y. Hu, R. Deng, R. Liang, W. Li, S. Liu and J. Zhu, *Langmuir*, 2013, **29**, 8825–8834.
- 37 Y. Zhu, H. Xuan, J. Ren, X. Liu and L. Ge, *ChemNanoMat*, 2016, **2**, 791–795.
- 38 P. Liu, J. Chen, Z. Zhang, Z. Xie, X. Du and Z. Gu, *Nanoscale*, 2018, **10**, 3673–3679.
- 39 Z. Shen, Y. Yang, F. Lu, B. Bao and B. You, *Polym. Chem.*, 2012, **3**, 2495–2501.
- 40 I. Jurewicz, A. A. K. King, R. Shanker, M. J. Large, R. J. Smith, R. Maspero, S. P. Ogilvie, J. Scheerder, J. Han, C. Backes, J. M. Razal, M. Florescu, J. L. Keddie, J. N. Coleman and A. B. Dalton, *Adv. Funct. Mater.*, 2020, 2002473.
- 41 J. Liao, C. Zhu, B. Gao, Z. Zhao, X. Liu, L. Tian, Y. Zeng, X. Zhou, Z. Xie and Z. Gu, *Adv. Funct. Mater.*, 2019, **29**, 1902954.
- 42 B. Yi and H. Shen, *J. Mater. Chem. C*, 2017, **5**, 8194–8200.
- 43 X. Su, Y. Jiang, X. Sun, S. Wu, B. Tang, W. Niu and S. Zhang, *Nanoscale*, 2017, **9**, 17877–17883.
- 44 F. Wang, X. Zhang, L. Zhang, M. Cao, Y. Lin and J. Zhu, *Dyes Pigm.*, 2016, **130**, 202–208.
- 45 Q. Zeng, C. Ding, Q. Li, W. Yuan, Y. Peng, J. Hu and K.-Q. Zhang, *RSC Adv.*, 2017, **7**, 8443–8452.
- 46 Y. Li, X. Wang, M. Hu, L. Zhou, L. Chai, Q. Fan and J. Shao, *Langmuir*, 2019, **35**, 14282–14290.
- 47 E. P. A. van Heeswijk, A. J. J. Kragt, N. Grossiord and A. Schenning, *Chem. Commun.*, 2019, **55**, 2880–2891.
- 48 X. Jia, J. Wang, K. Wang and J. Zhu, *Langmuir*, 2015, **31**, 8732–8737.
- 49 X. Jia, T. Zhang, J. Wang, K. Wang, H. Tan, Y. Hu, L. Zhang and J. Zhu, *Langmuir*, 2018, **34**, 3987–3992.
- 50 X.-Q. Wang, C.-F. Wang, Z.-F. Zhou and S. Chen, *Adv. Opt. Mater.*, 2014, **2**, 652–662.
- 51 L. R. Hart, J. L. Harries, B. W. Greenland, H. M. Colquhoun and W. Hayes, *Polym. Chem.*, 2013, **4**, 4860–4870.
- 52 S. Wang and M. W. Urban, *Nat. Rev. Mater.*, 2020, **5**, 562–583.
- 53 Y. T. Hsu, C. T. Tai, H. M. Wu, C. F. Hou, Y. M. Liao, W. C. Liao, G. Haider, Y. C. Hsiao, C. W. Lee, S. W. Chang, Y. H. Chen, M. H. Wu, R. J. Chou, K. P. Bera, Y. Y. Lin, Y. Z. Chen, M. Kataria, S. Y. Lin, C. R. P. Inbaraj, W. J. Lin, W. Y. Lee, T. Y. Lin, Y. C. Lai and Y. F. Chen, *ACS Nano*, 2019, **13**, 8977–8985.
- 54 B. Zhou, D. He, J. Hu, Y. Ye, H. Peng, X. Zhou, X. Xie and Z. Xue, *J. Mater. Chem. A*, 2018, **6**, 11725–11733.
- 55 R. Zheng, Y. Wang, C. Jia, Z. Wan, J. Luo, H. A. Malik, X. Weng, J. Xie and L. Deng, *ACS Appl. Mater. Interfaces*, 2018, **10**, 35533–35538.
- 56 X. Yan, Z. Liu, Q. Zhang, J. Lopez, H. Wang, H. C. Wu, S. Niu, H. Yan, S. Wang, T. Lei, J. Li, D. Qi, P. Huang, J. Huang, Y. Zhang, Y. Wang, G. Li, J. B. Tok, X. Chen and Z. Bao, *J. Am. Chem. Soc.*, 2018, **140**, 5280–5289.
- 57 Z. Deng, H. Wang, P. X. Ma and B. Guo, *Nanoscale*, 2020, **12**, 1224–1246.
- 58 H. Tan, Q. Lyu, Z. Xie, M. Li, K. Wang, K. Wang, B. Xiong, L. Zhang and J. Zhu, *Adv. Mater.*, 2019, **31**, 1805496.
- 59 J. Zhou, P. Han, M. Liu, H. Zhou, Y. Zhang, J. Jiang, P. Liu, Y. Wei, Y. Song and X. Yao, *Angew. Chem., Int. Ed.*, 2017, **56**, 10462–10466.
- 60 Y. Zhang, Y. Wang, Y. Wen, Q. Zhong and Y. Zhao, *ACS Appl. Mater. Interfaces*, 2020, **12**, 7486–7493.
- 61 M. Li, B. Zhou, Q. Lyu, L. Jia, H. Tan, Z. Xie, B. Xiong, Z. Xue, L. Zhang and J. Zhu, *Mater. Chem. Front.*, 2019, **3**, 2707–2715.
- 62 B. Yi and H. F. Shen, *Appl. Surf. Sci.*, 2018, **427**, 1129–1136.
- 63 J. Chen, L. Xu, M. Yang, X. Chen, X. Chen and W. Hong, *Chem. Mater.*, 2019, **31**, 8918–8926.
- 64 R. Hong, Y. Shi, X.-Q. Wang, L. Peng, X. Wu, H. Cheng and S. Chen, *RSC Adv.*, 2017, **7**, 33258–33262.
- 65 D. Ge, E. Lee, L. Yang, Y. Cho, M. Li, D. S. Gianola and S. Yang, *Adv. Mater.*, 2015, **27**, 2489–2495.
- 66 G. H. Lee, S. H. Han, J. B. Kim, J. H. Kim, J. M. Lee and S.-H. Kim, *Chem. Mater.*, 2019, **31**, 8154–8162.
- 67 G. H. Lee, J. B. Kim, T. M. Choi, J. M. Lee and S. H. Kim, *Small*, 2019, **15**, 1804548.
- 68 S. Y. Leo, W. Zhang, Y. Zhang, Y. Ni, H. Jiang, C. Jones, P. Jiang, V. Basile and C. Taylor, *Small*, 2018, **14**, 1703515.
- 69 G. I. Dzhardimalieva, B. C. Yadav, S. Singh and I. E. Uflyand, *Dalton Trans.*, 2020, **49**, 3042–3087.
- 70 C. H. Li and J. L. Zuo, *Adv. Mater.*, 2019, **32**, 1903762–1903790.
- 71 M. M. Perera and N. Ayres, *Polym. Chem.*, 2020, **11**, 1410–1423.
- 72 A. J. R. Amaral and G. Pasparakis, *Polym. Chem.*, 2017, **8**, 6464–6484.
- 73 C. H. Li and J. L. Zuo, *Adv. Mater.*, 2019, **32**, 1903762–1903790.
- 74 Y. Yang, D. Davydovich, C. C. Hornat, X. Liu and M. W. Urban, *Chem*, 2018, **4**, 1928–1936.
- 75 S. Bode, R. K. Bose, S. Matthes, M. Ehrhardt, A. Seifert, F. H. Schacher, R. M. Paulus, S. Stumpf, B. Sandmann, J. Vitz, A. Winter, S. Hoeppener, S. J. Garcia, S. Spange, S. van der Zwaag, M. D. Hager and U. S. Schubert, *Polym. Chem.*, 2013, **4**, 4966–4973.
- 76 G. A. Williams, R. Ishige, O. R. Cromwell, J. Chung, A. Takahara and Z. Guan, *Adv. Mater.*, 2015, **27**, 3934–3941.
- 77 Z. Chen, J. Wu, Y. Wang, C. Shao, J. Chi, Z. Li, X. Wang and Y. Zhao, *Small*, 2019, **15**, 1903104.
- 78 F. Fu, Z. Chen, Z. Zhao, H. Wang, L. Shang, Z. Gu and Y. Zhao, *Proc. Natl. Acad. Sci. U. S. A.*, 2017, **11**, 5900–5905.
- 79 F. Meng, M. M. Umair, K. Iqbal, X. Jin, S. Zhang and B. Tang, *ACS Appl. Mater. Interfaces*, 2019, **11**, 13022–13028.
- 80 X. Wang, Y. Qiu, G. Chen, Z. Chu, A. Shadike, C. Chen, C. Chen and Z. Zhu, *ACS Appl. Polym. Mater.*, 2020, **2**, 2086–2092.
- 81 S.-N. Yin, J. Liu, D. Wu, S. Chen and W. Xia, *ACS Appl. Polym. Mater.*, 2019, **2**, 448–454.

- 82 M. Li, H. Tan, L. Jia, R. Zhong, B. Peng, J. Zhou, J. Xu, B. Xiong, L. Zhang and J. Zhu, *Adv. Funct. Mater.*, 2020, **30**, 2000008.
- 83 M. Li, Q. Lyu, J. Zhu and L. Zhang, *Acta Polym. Sin.*, 2019, **50**, 271–280.
- 84 L. Shi, Y. Zhang, B. Dong, T. Zhan, X. Liu and J. Zi, *Adv. Mater.*, 2013, **25**, 5314–5320.
- 85 M. Iwata, M. Teshima, T. Seki, S. Yoshioka and Y. Takeoka, *Adv. Mater.*, 2017, **29**, 1605050–1605057.
- 86 Y. Meng, B. Tang, J. Cui, S. Wu, B. Ju and S. Zhang, *Adv. Mater. Interfaces*, 2016, **3**, 1600374.
- 87 Y. Hu, D. Yang and S. Huang, *ACS Omega*, 2019, **4**, 18771–18779.